

## Supplementary Information

### Section 1. General Characterizations

#### Crystal date of Cd-MOF

Table S1 Selective Bond lengths [Å] and angles [°] for Cd-MOF.

Cd(1)-N(1)	2.2367(15)	Cd(1)-O(2)	2.2393(13)
Cd(1)-N(3)	2.3095(16)	Cd(1)-O(4)#1	2.3465(15)
Cd(1)-O(3)#1	2.4139(15)	Cd(1)-O(1)	2.5968(14)
N(1)-Cd(1)-O(2)	129.90(6)	N(1)-Cd(1)-N(3)	94.22(6)
O(2)-Cd(1)-N(3)	98.99(5)	N(1)-Cd(1)-O(4)#1	128.75(6)
O(2)-Cd(1)-O(4)#1	100.50(5)	N(3)-Cd(1)-O(4)#1	85.22(5)
N(1)-Cd(1)-O(3)#1	100.95(6)	O(2)-Cd(1)-O(3)#1	100.94(6)
N(3)-Cd(1)-O(3)#1	137.53(5)	O(4)#1-Cd(1)-O(3)#1	54.48(5)
N(1)-Cd(1)-O(1)	82.76(5)	O(2)-Cd(1)-O(1)	53.19(5)
N(3)-Cd(1)-O(1)	132.30(6)	O(4)#1-Cd(1)-O(1)	132.59(5)
O(3)#1-Cd(1)-O(1)	89.16(5)		

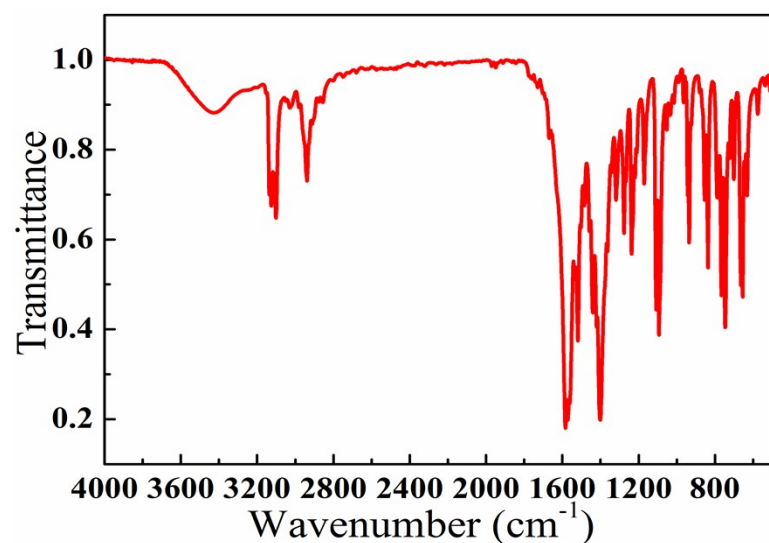
Symmetry code: #1 x+1, y, z

## Section 2. Comparison

**Table S2.**

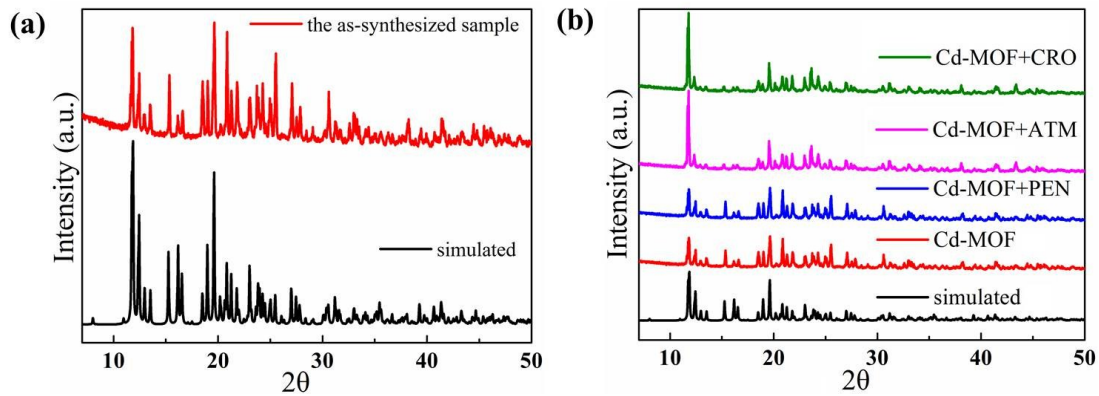
Journal	MOFs	$K_{sv}$ ( $M^{-1}$ )	Antibiotic type	LOD	Reference
<i>J Am Chem Soc</i>	Zr(IV)-based MOFs	$1.1 \times 10^5$	12	58 ppb	[1]
<i>J. Mater. Chem. A</i>	Cd(II)-based MOFs	$1.33 \times 10^5$	9	60 ppb	[2]
<i>Anal Chem</i>	In-MOFs	---	10	0.2 ppm	[3]
<i>Crystal growth &amp; Design</i>	Zn/Cd-MOFs	$4.063 \times 10^4$	11	0.90 $\mu M$	[4]

## Section 3. FT-IR spectrum of Cd-MOF

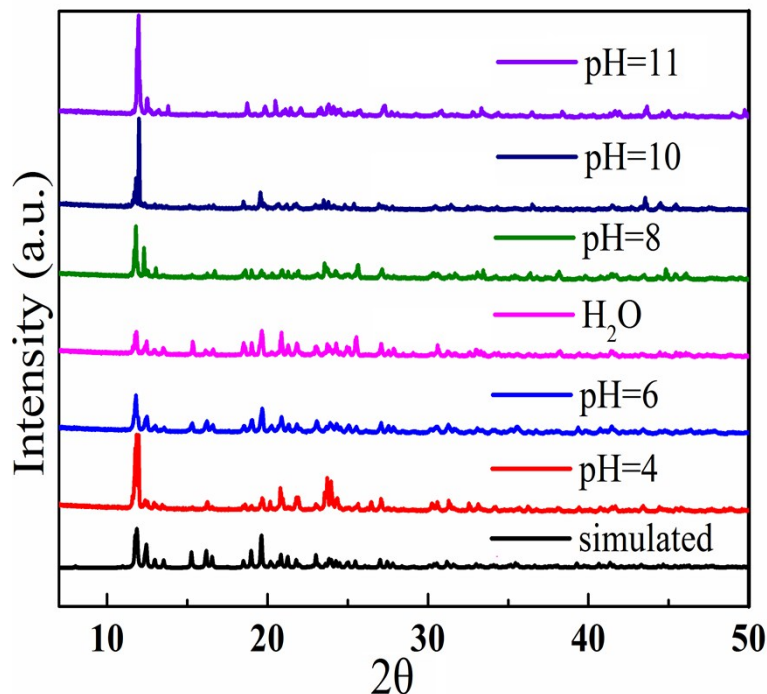


**Fig. S1:** FT-IR spectrum of Cd-MOF

## Section 4. PXRD patterns

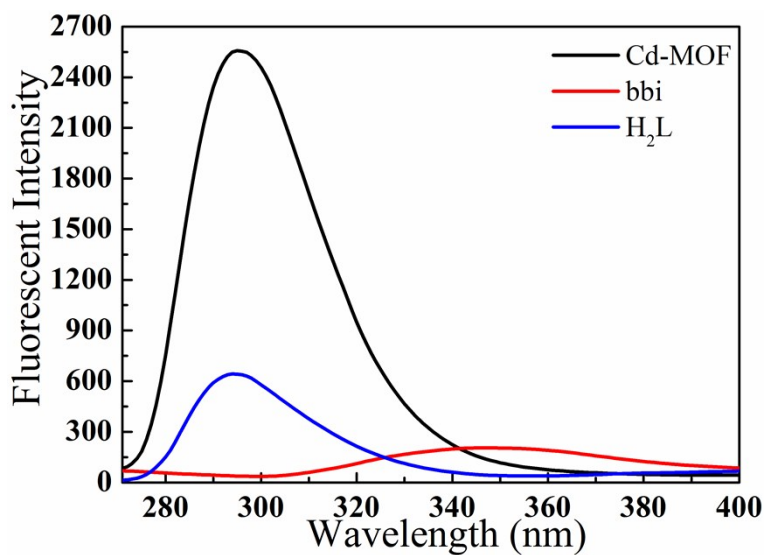


**Fig. S2:** (a) The PXRD pattern of the as-synthesised sample(Cd-MOF); (b) The PXRD pattern of Cd-MOF immersed in antibiotic solution(14  $\mu$ M).



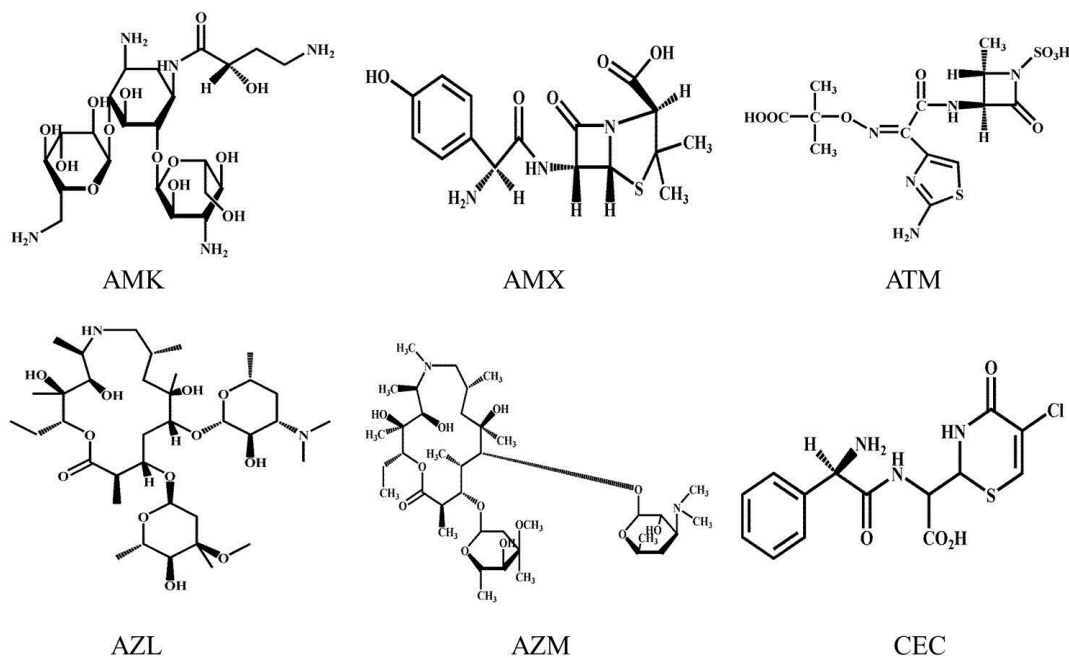
**Fig. S3:** The PXRD pattern of Cd-MOF immersed in pH= 4, 6, 8, 10, 11 aqueous solutions and  $H_2O$  for 24 h.

**Section 5.** The fluorescence spectra of solid samples



**Fig. S4:** The fluorescence spectra of solid samples of Cd-MOF, bbi and H<sub>2</sub>L ligands.

## Section 6. The structural figure of antibiotics



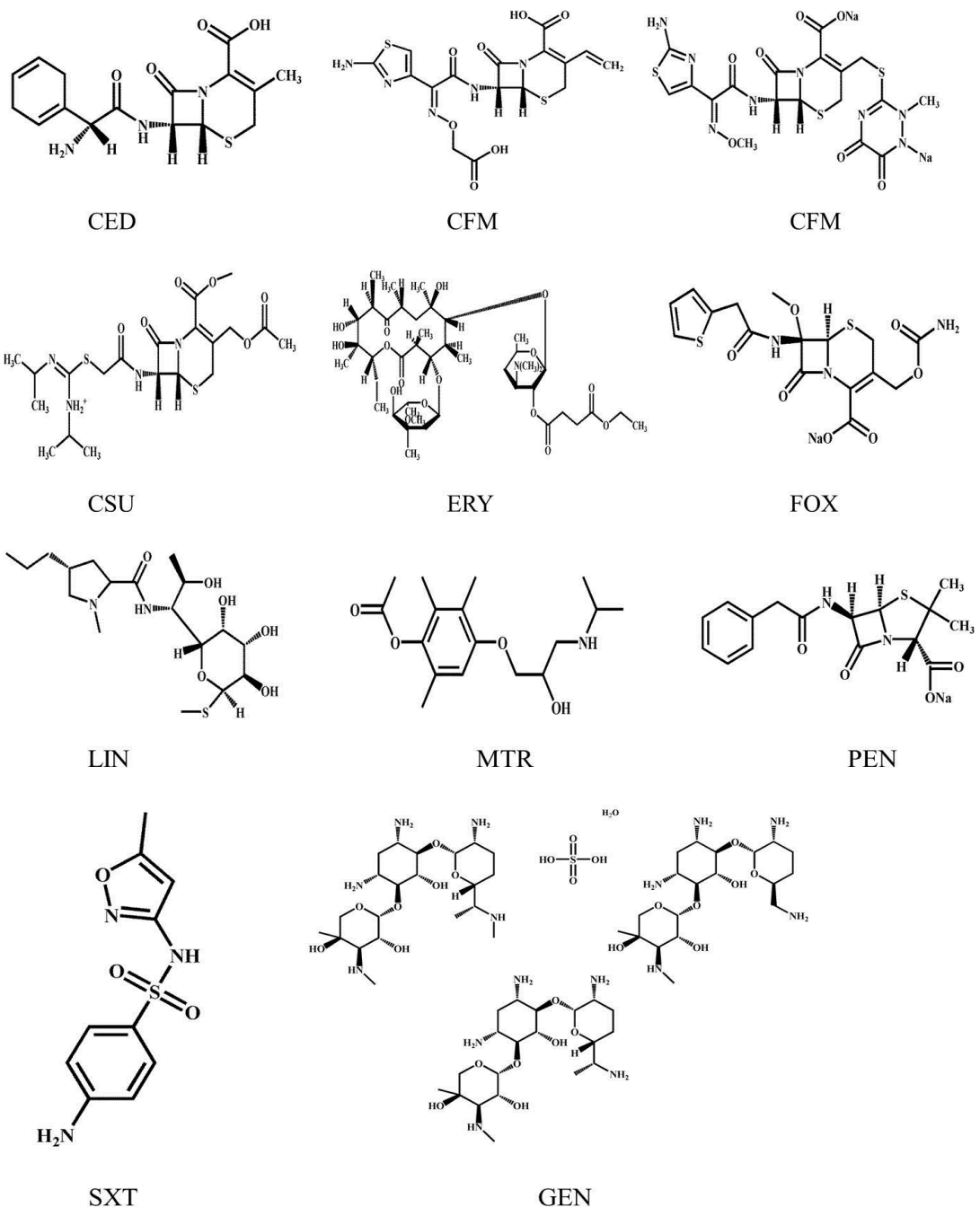


**Fig. S5:** The structural figure of antibiotics

## Section 7. UV-vis and FL spectra of ligands

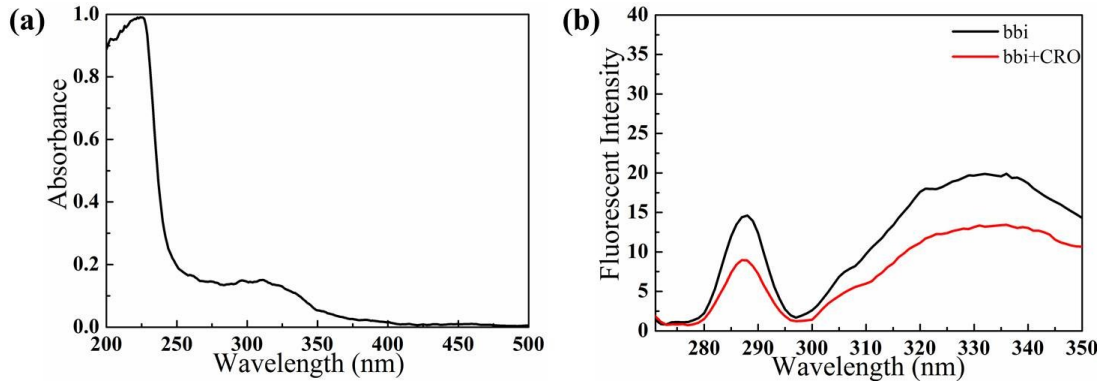


**Fig. S6:** (a) UV–vis absorbance spectra of bbi; (b) The fluorescent spectra of a aqueous solution of bbi and CRO(14  $\mu\text{M}$ ) added to aqueous solution of bbi.

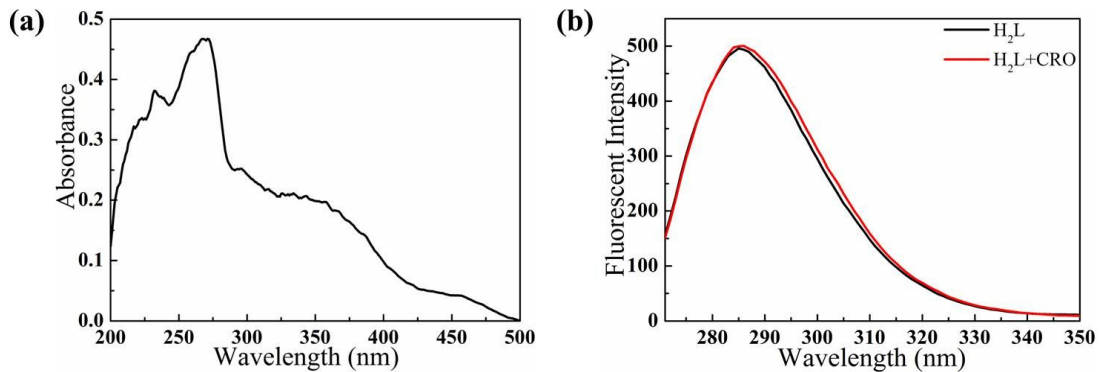


**Fig. S7:** (a) UV–vis absorbance spectra of  $\text{H}_2\text{L}$ ; (b) The fluorescent spectra of aqueous solution of  $\text{H}_2\text{L}$  and CRO (14  $\mu\text{M}$ ) added to aqueous solution of  $\text{H}_2\text{L}$ .

## Section 8. The recyclability tests

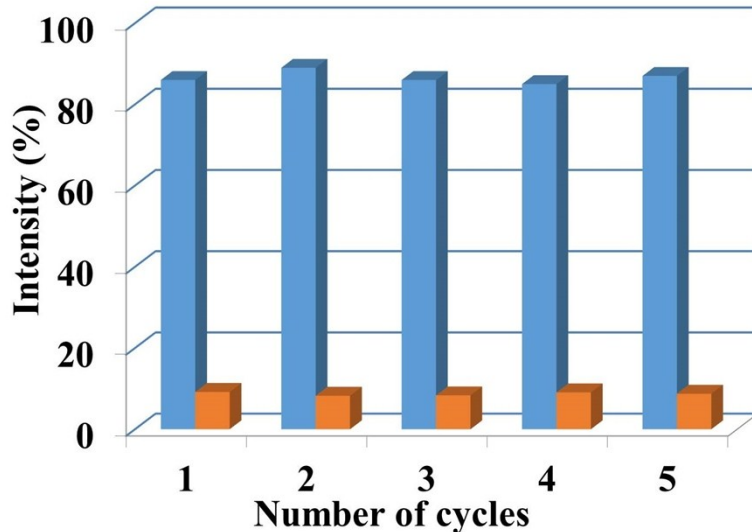


**Fig. S8:** The recyclability tests of Cd-MOFs in CRO(14  $\mu\text{M}$ ) solution. The blue columns represent the initial relative luminescent intensity and the yellow columns represent the relative intensity on addition of CRO.

## Section 9. Detection of selected antibiotics

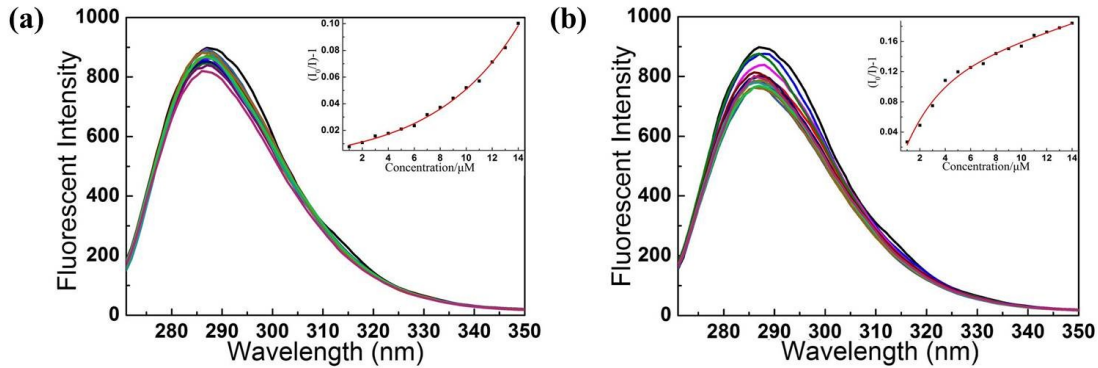


**Fig. S9:** The fluorescent spectra of Cd-MOF dispersed in water upon incremental addition of 70  $\mu$ L (1 mM, 5  $\mu$ L addition each time) aqueous solution of (a) SXT (b) ATM, respectively (the corresponding calibration curve of Stern-Volmer plot).

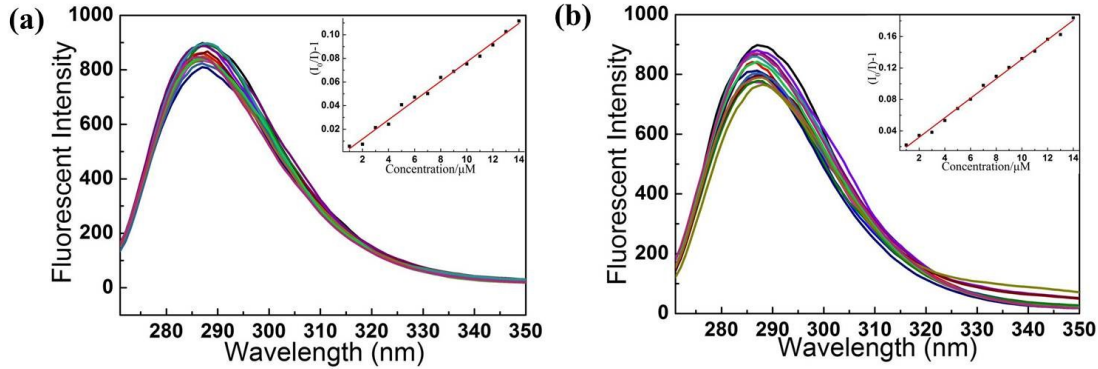


**Fig. S10:** The fluorescent spectra of Cd-MOF dispersed in water upon incremental addition of 70  $\mu$ L (1 mM, 5  $\mu$ L addition each time) aqueous solution of (a) AMX (b) CFM, respectively (the corresponding calibration curve of Stern-Volmer plot).

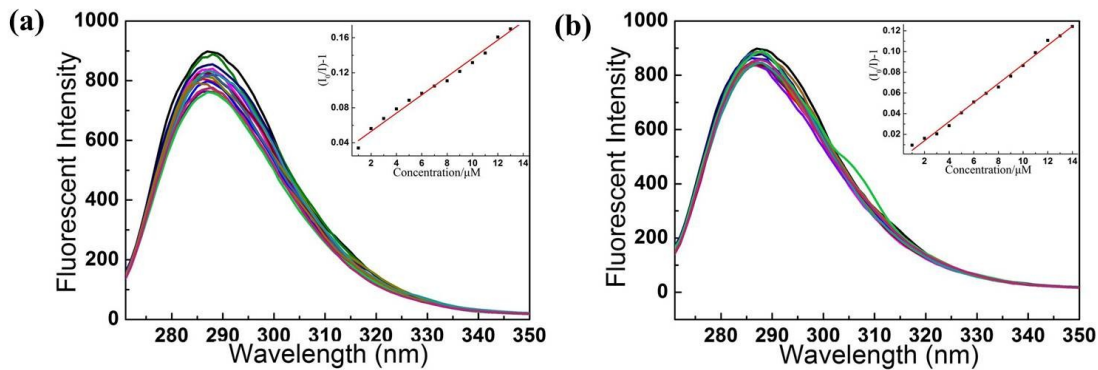


**Fig. S11:** The fluorescent spectra of Cd-MOF dispersed in water upon incremental addition of 70  $\mu$ L (1 mM, 5  $\mu$ L addition each time) aqueous solution of (a) CED (b) AZM, respectively (the corresponding calibration curve of Stern-Volmer plot).

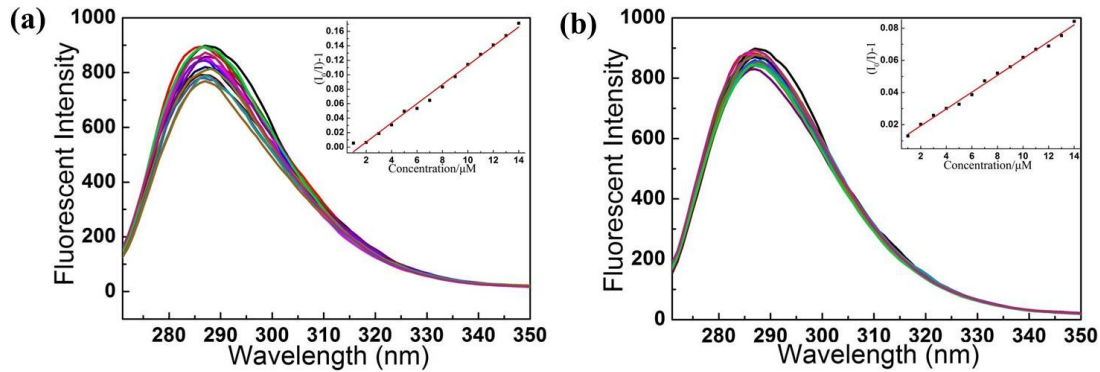


**Fig. S12:** The fluorescent spectra of Cd-MOF dispersed in water upon incremental addition of 70  $\mu$ L (1 mM, 5  $\mu$ L addition each time) aqueous solution of (a) CEC (b) PEN, respectively (the corresponding calibration curve of Stern-Volmer plot).

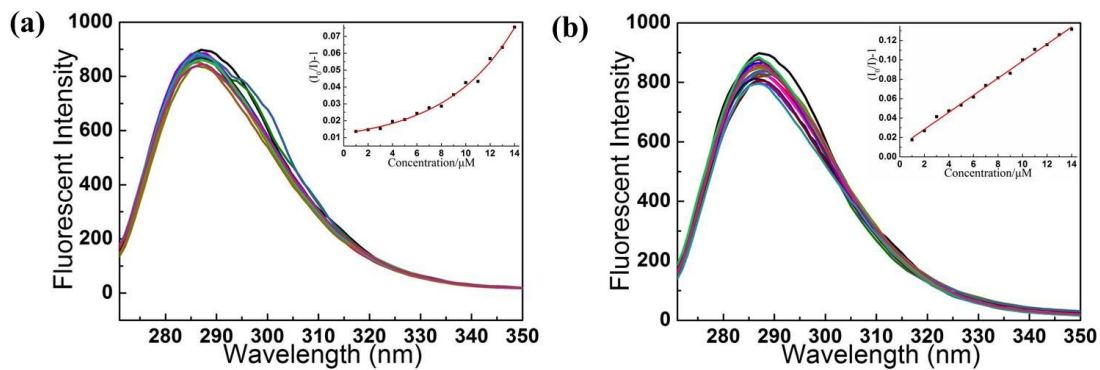


**Fig. S13:** The fluorescent spectra of Cd-MOF dispersed in water upon incremental addition of 70  $\mu$ L (1 mM, 5  $\mu$ L addition each time) aqueous solution of (a) AZL (b) FOX, respectively (the corresponding calibration curve of Stern-Volmer plot).

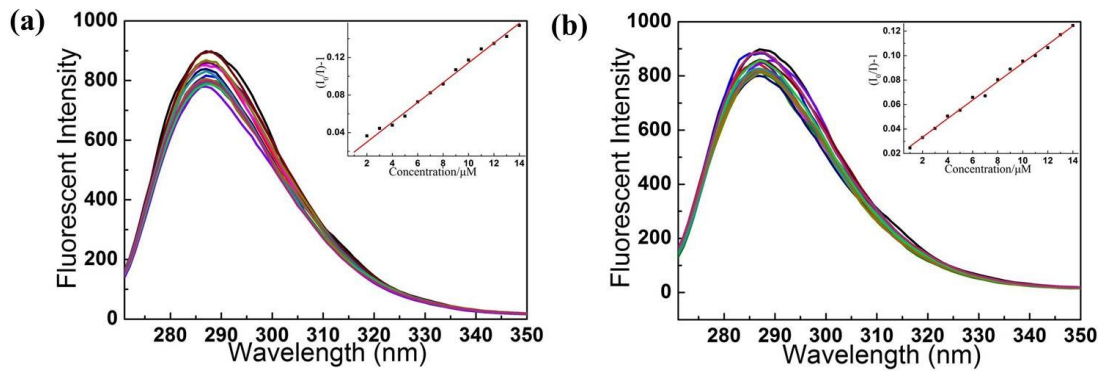


**Fig. S14:** The fluorescent spectra of Cd-MOF dispersed in water upon incremental addition of 70  $\mu$ L (1 mM, 5  $\mu$ L addition each time) aqueous solution of (a) CSU (b) ATM, respectively (the corresponding calibration curve of Stern-Volmer plot).

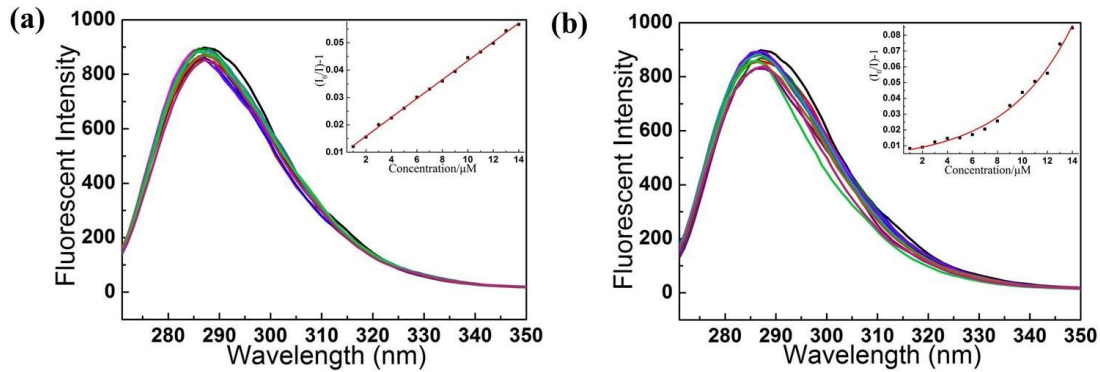


**Fig. S15:** The fluorescent spectra of Cd-MOF dispersed in water upon incremental addition of 70  $\mu\text{L}$  (1 mM, 5  $\mu\text{L}$  addition each time) aqueous solution of (a) LIN (b) AMK, respectively (the corresponding calibration curve of Stern-Volmer plot).

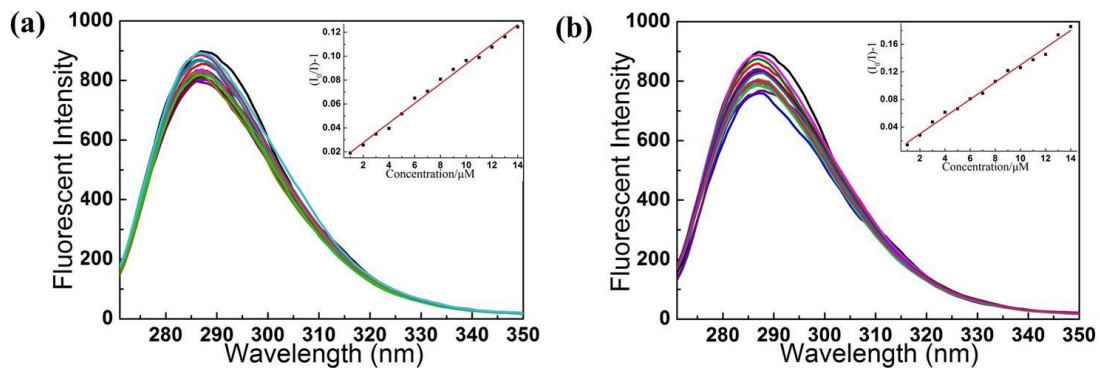


**Figure S16.** The fluorescent spectra of Cd-MOF dispersed in water upon incremental addition of 70  $\mu\text{L}$  (1 mM, 5  $\mu\text{L}$  addition each time) aqueous solution of (a) GEN (b) SXT, respectively (the corresponding calibration curve of Stern-Volmer plot).

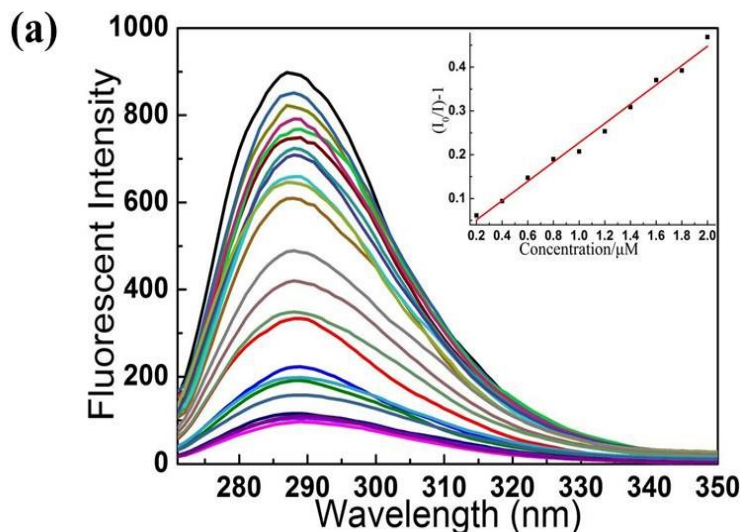


**Figure S17.** The fluorescent spectra of Cd-MOF dispersed in water upon incremental addition of 70  $\mu\text{L}$  (1  $\mu\text{L}$  each time to 10  $\mu\text{L}$ , then 5  $\mu\text{L}$  each time to 70  $\mu\text{L}$ ) aqueous solution of (a) CRO (the corresponding calibration curve of Stern-Volmer plot).

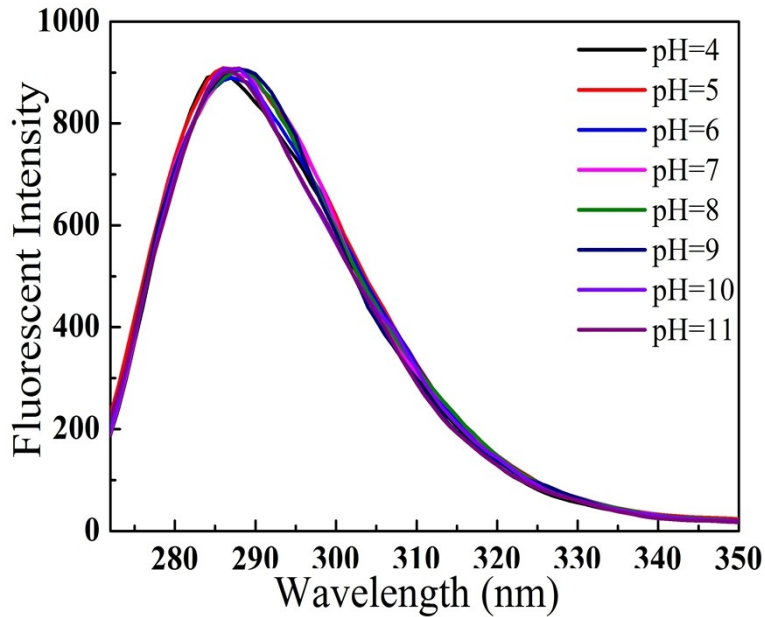


**Figure S18.** In pH=4~11 aqueous solutions, fluorescence intensity of Cd-MOF probe;

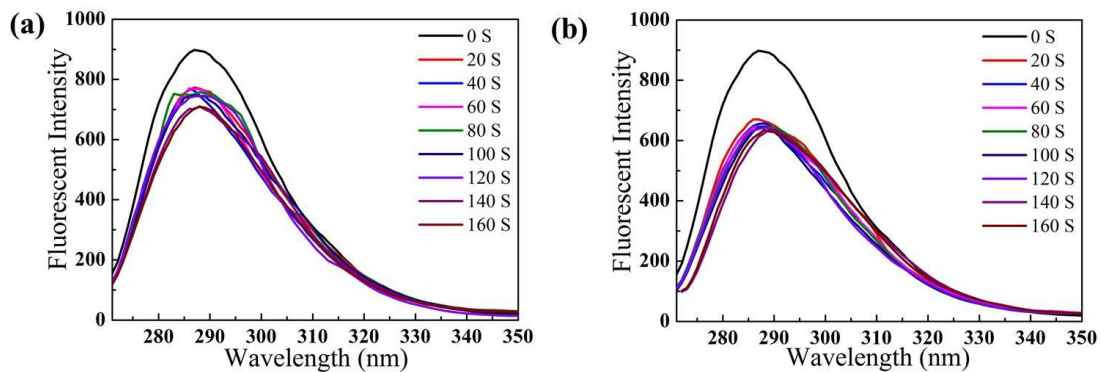


**Fig. S19:** CRO (a.1  $\mu\text{M}$ , b, 1.6  $\mu\text{M}$ ) added to Cd-MOF suspensions, fluorescence intensity time curve.

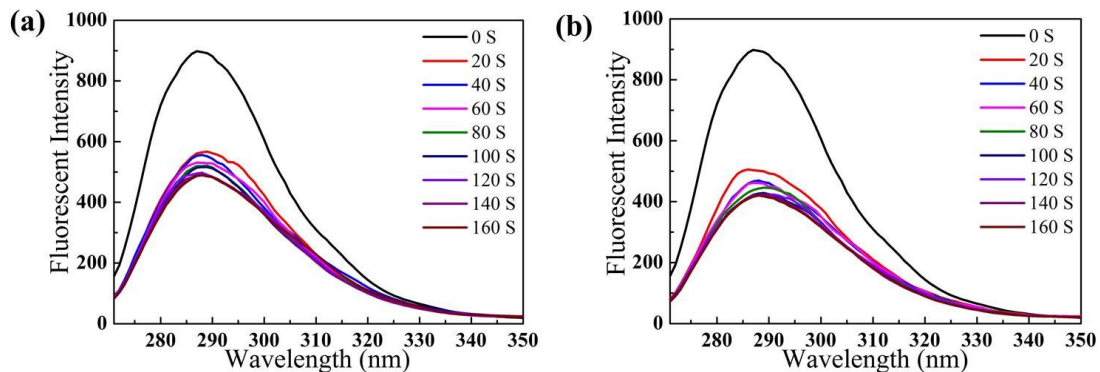


**Fig. S20:** CRO (a.2  $\mu\text{M}$ , b, 3  $\mu\text{M}$ ) added to Cd-MOF suspensions, fluorescence intensity time curve.

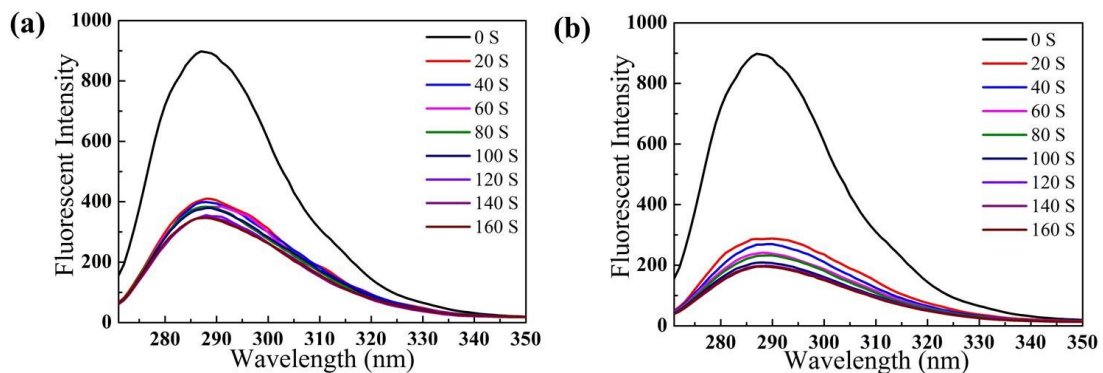


**Fig. S21:** CRO (a. 4  $\mu\text{M}$ , b, 6  $\mu\text{M}$ ) added to Cd-MOF suspensions, fluorescence intensity time curve.

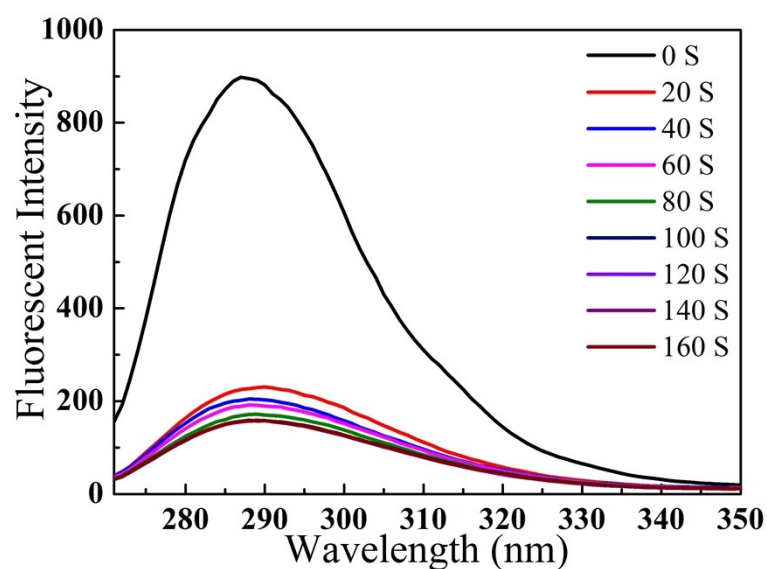


**Fig. S22:** CRO(8  $\mu\text{M}$ ) added to Cd-MOF suspensions, fluorescence intensity time curve.

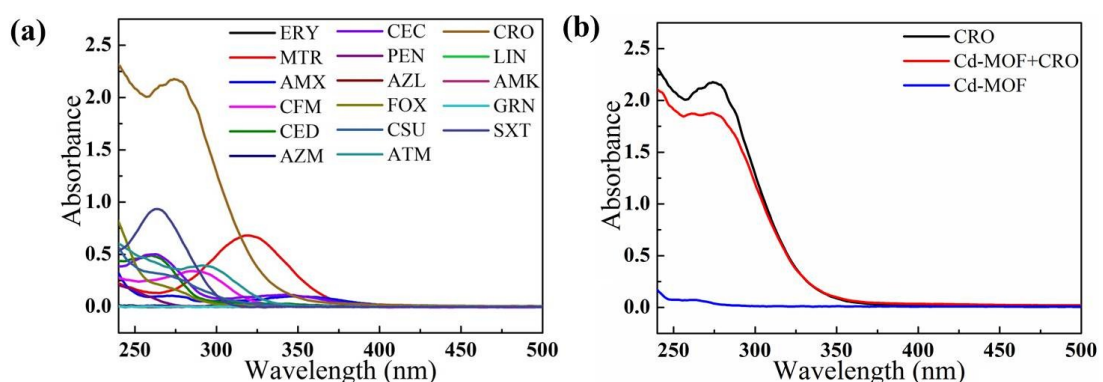


**Fig. S23:** (a) UV-visible spectra of antibiotics in water; (b) UV-visible spectra of CRO, Cd-MOF, mixtures of CRO and Cd-MOF in water.

#### **4. References**

- 1 B. Wang, X.L Lv, D.W. Feng, L.H. Xie, J. Zhang, M. Li, Y.B. Xie, J.R. Li, H.C. Zhou, Highly Stable Zr(IV)-Based Metal-Organic Frameworks for the Detection and Removal of Antibioticsand Organic Explosives in Water, *J Am Chem Soc*, 2016, 138(19), 6204-6216.
- 2 D. Zhao, X.H. Liu, Y. Zhao, P. Wang, Y. Liu, M. Azam, SI. Al-Resayes, Y. Lu, W.Y. Sun, Luminescent Cd(II)-organic frameworks with chelating NH<sub>2</sub> sites for selective detection of Fe(III) and antibiotics, *J Am Chem Soc*, 2017, 5(30) 15797-15807.
- 3 S.L. Hou, J. Dong, X.L. Jiang, Z.H. Jiao, C.M. Wang, B. Zhao, Interpenetration-Dependent Luminescent Probe in Indium-Organic Frameworks for Selectively Detecting Nitrofurazone in Water, *Anal Chem*, 2018, 90(3)1516-1519.
- 4 Z.W. Zhai, S.H. Yang, M. Cao, L.K. Li, C.X. Du, S.Q. Zang, Rational Design of Three Two-Fold Interpenetrated Metal-Organic Frameworks: Luminescent Zn/Cd-Metal-Organic Frameworks for Detection of 2,4,6-Trinitrophenol and Nitrofurazone in the Aqueous Phase, *Crystal Growth & Design*, 2018, 18(11) 7173-7182.